ACS Biomaterials SCIENCE & ENGINEERING

pubs.acs.org/journal/abseba

Article

A Defined and Scalable Peptide-Based Platform for the Generation of Human Pluripotent Stem Cell-Derived Astrocytes

Sreedevi Raman,[§] Gayathri Srinivasan,[§] Nicholas Brookhouser,[§] Toan Nguyen, Tanner Henson, Daylin Morgan, Joshua Cutts, and David A. Brafman*

Cite This: *ACS Biomater. Sci. Eng.* 2020, 6, 3477−3490

Read Online

ACCESS | Metrics & More | Article Recommendations | Supporting Information

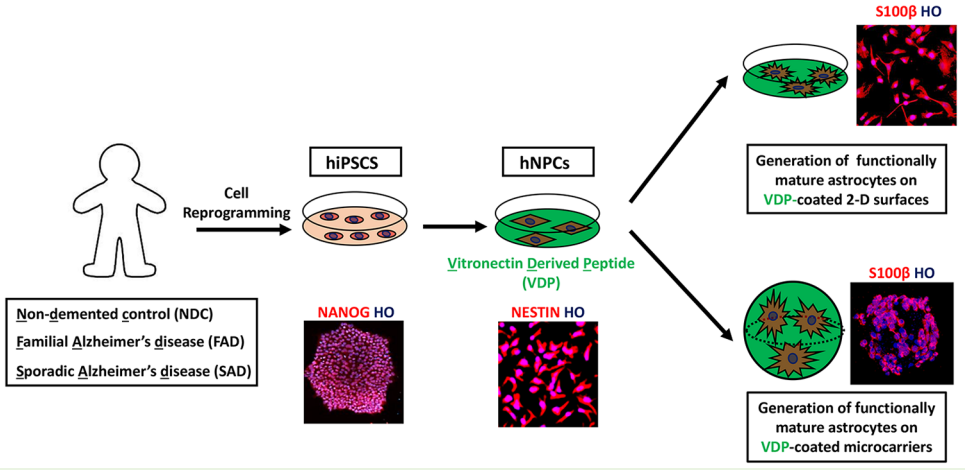

ABSTRACT: Astrocytes comprise the most abundant cell type in the central nervous system (CNS) and play critical roles in maintaining neural tissue homeostasis. In addition, astrocyte dysfunction and death has been implicated in numerous neurological disorders such as multiple sclerosis, Alzheimer's disease, amyotrophic lateral sclerosis (ALS), and Parkinson's disease (PD). As such, there is much interest in using human pluripotent stem cell (hPSC)-derived astrocytes for drug screening, disease modeling, and regenerative medicine applications. However, current protocols for generation of astrocytes from hPSCs are limited by the use of undefined xenogeneic components and two-dimensional (2D) culture surfaces, which limits their downstream applications where large-quantities of cells generated under defined conditions are required. Here, we report the use of a completely synthetic, peptide-based substrate that allows for the differentiation of highly pure populations of astrocytes from several independent hPSC lines, including those derived from patients with neurodegenerative disease. This substrate, which we demonstrate is compatible with both conventional 2D culture formats and scalable microcarrier (MC)-based technologies, leads to the generation of cells that express high levels of canonical astrocytic markers as well as display properties characteristic of functionally mature cells including production of apolipoprotein E (ApoE), responsiveness to inflammatory stimuli, ability to take up amyloid-β (Aβ), and appearance of robust calcium transients. Finally, we show that these astrocytes can be cryopreserved without any loss of functionality. In the future, we anticipate that these methods will enable the development of bioprocesses for the production of hPSC-derived astrocytes needed for biomedical research and clinical applications.

KEYWORDS: *Human pluripotent stem cells, astrocytes, peptide, defined conditions, biomanufacturing, neurodegenerative disease*

INTRODUCTION

Astrocytes are an abundant, specialized non-neuronal cell type in the central nervous system (CNS) that have numerous functions in maintaining healthy neural tissue including axonal development and guidance, synapse formation and function, ion and neurotransmitter balance, and energy metabolism.[1−4] In addition, astrocytes are important mediators in response to traumatic injury and infectious agents.[4,5] Moreover, death or dysregulation of astrocytes has been implicated in numerous CNS pathologies and disorders such as multiple sclerosis, Alzheimer's disease (AD), amyotrophic lateral sclerosis (ALS),

Received: January 15, 2020
Accepted: May 6, 2020
Published: May 6, 2020

and Parkinson's disease.[3] Because of the diverse roles that astrocytes play in CNS homeostasis and disease, there is a critical need for models to study astrocyte biology *in vitro* and strategies to replace diseased astrocytes *in vivo*.

Advances in cellular reprogramming have allowed for the generation of human induced pluripotent stem cells (hPSCs) that can be used to dissect disease mechanisms on a cellular level, evaluate potential therapeutics on human cells with euploid karyotypes, and provide the unlimited raw material for cell-based therapies. Specifically, hPSC-derived astrocytes have allowed for the study of a variety of neurodegenerative diseases in a simplified and accessible system.[6] In addition, astrocytes generated from hPSCs have enabled a variety of novel neurotoxicity and drug screening paradigms.[7,8] Finally, astrocytic populations produced from hPSCs have shown promise in replacing the diseased and damaged tissue in conditions such as ALS, stroke, and AD.[9−11]

Despite these advances, according to several technology road maps developed by the regenerative medicine industry, scalable and adaptable culture methods that employ cost-effective, chemically defined substrates are still needed to generate the large quantities of cells required for downstream applications in disease modeling, drug screening, and cell-based therapies.[12−15] More specifically, current biomanufacturing techniques are limited by the following. First, current differentiation protocols employ undefined substrates such as Matrigel[16] or extracellular matrix proteins (ECMPs) isolated from animal sources.[17−20] In turn, such heterogeneous xenogeneic components not only pose a risk of transmitting adventitious pathogens but also suffer from batch-to-batch variability, which might limit their compatibility with downstream clinical applications.[21,22] Second, conventional astrocyte generation strategies employ traditional two-dimensional (2D) culture techniques, which do not allow for production of large cell quantities needed for drug screening and cell-based therapies. For example, it has been estimated that 10^9 to 10^{10} cells will be required to screen a 1 million compound library or provide a single therapeutic dose,[23,24] which will not be achievable with typical 2D differentiation methods. Lastly, existing schemes require the differentiation of astrocytes in real-time immediately prior to their application and do not allow for their long-term storage to enable point of use.[25,26]

In previous work, we identified a completely synthetic substrate, termed vitronectin-derived peptide (VDP), that allowed for the long-term expansion and neuronal differentiation of multiple human neural progenitor cell (hNPC) lines.[27] Here, we significantly expand upon this work to use this peptide as a fully defined surface for the differentiation of astrocytes from multiple independent hPSC lines. We demonstrate that these cell populations express high levels of canonical astrocytic markers and display a genome-wide transcriptional profile that is indistinguishable from cells generated on conventional animal-derived ECMP-based surfaces. Moreover, these populations displayed properties of functionally mature astrocytes including production of apolipoprotein E (ApoE), responsiveness to inflammatory stimuli, ability to take up amyloid-β (Aβ), and presentation of robust calcium transients. In addition, we demonstrate that this defined peptide substrate is compatible with scalable microcarrier (MC)-based techniques. Finally, we establish that these astrocytes can be cryopreserved without any loss of functionality. Overall, the strategies developed here will enable biomanufacturing processes for the large-scale production and long-term storage of hPSC-derived astrocytes needed for downstream application in disease modeling, drug screening, and regenerative medicine.

MATERIALS AND METHODS

Synthesis of Vitronectin-Derived Peptide (VDP). Peptide synthesis was performed as we previously described.[35]

Human Neural Progenitor Cell (hNPC) Generation and Expansion. Human neural progenitor cells (hNPCs) were generated and cultured similar to the previously described methods.[27] Briefly, hNPCs were cultured on laminin (LN)- or VDP-coated tissue culture plates in the presence of neural expansion medium [NEM; 1× DMEM-F12 (Thermo Fisher), 0.5% (v/v) N2 supplement (Thermo Fisher), 1% (v/v) B27 supplement (Thermo Fisher), 1% (v/v) GlutaMAX supplement (Thermo Fisher), 1% (v/v) Penicillin Streptomycin (Thermo Fisher), 30 ng/mL FGF2 (STEMCELL Technologies), and 30 ng/mL EGF (STEMCELL Technologies)]. Every 3−4 days, hNPCs were enzymatically passaged with Accutase (Thermo Fisher) onto freshly coated LN or VDP plates.

Differentiation of hNPCs to Astrocytes on 2D Surfaces. hPSC-derived astrocytes were generated as previously described.[28] Briefly, astrocytes were differentiated for a minimum of 50 days (unless otherwise noted) on LN- or VDP-coated plates by culturing high passage (greater than passage 6) hNPCs in astrocyte differentiation medium [ADM; 1× complete astrocyte medium (ScienCell), 10 ng/mL human recombinant BMP4 (STEMCELL Technologies), 10 ng/mL human recombinant heregulin-β (STEMCELL Technologies), and 10 ng/mL human recombinant CNTF (STEMCELL Technologies)].

VDP and LN Coating of Microcarriers (MCs). MCs (Corning Enhanced Attachment Microcarriers) were coated with VDP or LN using methods similar to those previously described.[35]

Differentiation of hNPCs to Astrocytes on MCs. hNPCs were seeded on VDP-coated MCs in 6-well ultralow attachment plates (Corning) with 1.5×10^6 cells per well and 1 mg/mL MCs. The cells and MCs were suspended at half the final culture volume of 4 mL in NEM supplemented with 5 μM Rho kinase inhibitor (ROCKi Y-27632). The plates were then placed in the incubator for 12 h to allow for cell attachment. The rest of the media and ROCKi were added to the cultures after 12 h, and the cells were placed on an orbital shaker at 95 rpm; the cultures were agitated for the rest of the culture period. Twenty-four hours after seeding the hNPCs on MCs, the media was switched to ADM to start hNPC differentiation to astrocytes. Cells were maintained in ADM for 50 days with half media changes every day until further analysis or replating. Cells were removed from the MCs by incubating in a papain solution containing Earle's balanced salt solution (Alfa Aesar), 20 U/mL papain (Worthington), 1 mM L-cysteine, 22.5 mM D-glucose, 26 mM $NaHCO_3$, and 125 U/mL DNase (Roche) for 20 min at 37 °C and then triturated with an inhibitor solution containing 1 mg/mL ovomucoid inhibitor (Roche) and 1 mg/mL BSA (Sigma).[29] A 40 μm cell strainer was used to separate the cells from the MCs, and the cells were seeded on freshly coated VDP MCs.

Differentiation of hNPCs to Neurons on Microcarriers. hNPCs were differentiated to neurons on MCs as previously described.[35] hNPCs were differentiated on MCs for a minimum of 30 days before further analysis or replating.

Flow Cytometry Analysis. Cells were processed for flow cytometry analysis using an ACCURI C6 (BD Biosciences) as previously described.[35] For viability assessment, cells were stained with 0.01 mg/mL propidium iodide (Thermo Fisher) in PBS. Supplementary Table 1 lists antibodies and isotype negative controls used in this study.

Quantitative PCR (qPCR). Gene expression was measured using qPCR and normalized to 18S rRNA levels as described previously.[35] The list of specific primer sequences that were employed in qPCR analysis is provided in Supplementary Table 2.

Immunofluorescence. Immunofluorescence staining of cells on 2D and MC surfaces as well as subsequent image analysis was

https://dx.doi.org/10.1021/acsbiomaterials.0c00067
ACS Biomater. Sci. Eng. 2020, 6, 3477−3490

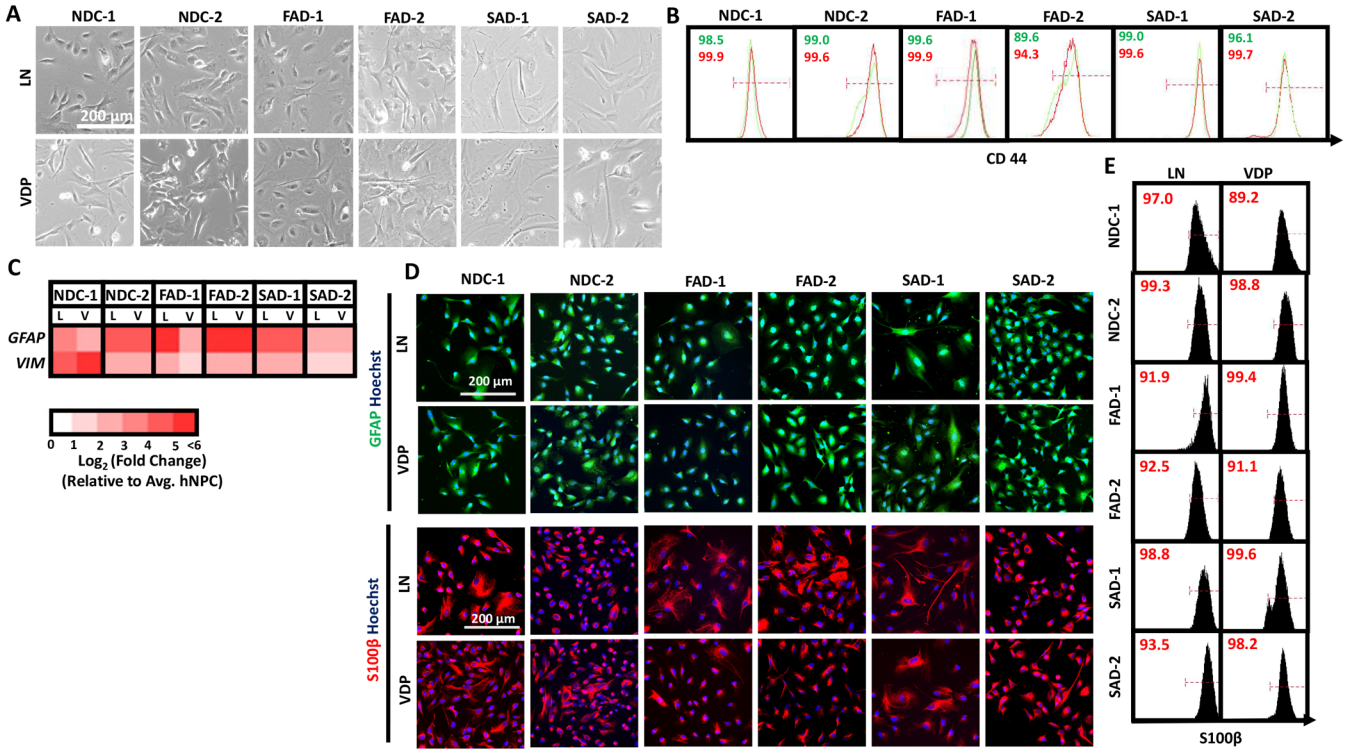

Figure 1. Generation of hPSC-derived astrocytes on a completely synthetic peptide substrate. (A) Representative phase contrast images of D50+ hPSC-derived astrocytes generated (scale bar = 200 μm). (B) Representative flow cytometry plots of CD44 expression of D30+ astrocytes on VDP (green traces) and LN (red traces) substrates. Gates were determined using isotype antibody only controls listed in Supplementary Table 1. (C) Quantitative PCR (qPCR) analysis for expression of astrocyte markers *GFAP* and *VIM* in D50+ cultures. Gene expression fold changes were calculated relative to expression levels in undifferentiated hNPCs. (D) Immunofluorescence analysis for expression of GFAP and S100β in D50+ cultures. (E) Representative flow cytometry plots of S100β expression of D50+ astrocytes. Gates were determined using isotype or secondary antibody only controls listed in Supplementary Table 1.

performed as previously described.[35] Primary and secondary antibodies that were used are listed in Supplementary Table 1. All images were acquired on an automated confocal microscope (Leica TCS SP5) or EVOS microscope.

RNA-seq Analysis. All sequencing was performed at BGI Americas Corporation using BGISEQ-500 for a single end 50 bp run as described previously.[35] Reads were subsequently mapped to the hg19 human reference genome using STAR 2.5.2b.[30] Differential analysis was performed using gene counts obtained from featureCounts[31] in EdgeR.[32] Gene ontology analysis was performed using lists of differentially expressed genes in DAVID.[33]

Cytokine Bead Array. Astrocytes were seeded in a 24 well plate at a density of 25 × 10^3 cells per well. Three days later, cells were treated with 25 μg/mL lipopolysaccharide (Thermo Fisher) for 24 h as previously described.[34] The cell supernatant was collected after lipopolysaccharide treatment, stored at −20 °C, and thawed on ice before cytokine analysis using the LEGENDplex Human Inflammation Panel (Biolegend) as directed by the manufacturer. The samples were subsequently analyzed on an Attune NxT flow cytometer (ThermoFisher), and cytokine concentration was determined using the LEGENDplex data analysis software.

Apolipoprotein E (ApoE) ELISA. Astrocytes were seeded in a 12 well plate at a density of 1 × 10^5 cells per well. Three days later, the cell supernatant was concentrated using Amicon Ultra filters (EMD Millipore) and stored at −80 °C until analysis. ApoE levels in the medium were measured with the Human ApoE (AD2) ELISA Kit (Thermo Scientific).

Calcium Imaging. For calcium imaging analysis, astrocytes were seeded at a density of 2 × 10^5 in a glass 40 mm dish. Cells were incubated with 2 μM Fluo-4 AM (ThermoFisher) and 0.02% Pluronic F-127 in DMEM for 15 min at 37 °C. After one wash in HEPES-buffered Tyrode's solution (Alfa Aesar), the dye was allowed to de-esterify by incubating the cells at room temperature for 20 min prior to imaging on a Zeiss AxioObserver Z1. Fluorescent time-lapse images were acquired (20× objective) at 1 s intervals for 360 s. Calcium spike traces were generated by quantifying the mean pixel intensity of manually identified regions of interest using the ImageJ software. For astrocytes cultured on microcarriers, cells differentiated for at least 45 days were replated at a density of 1.4 × 10^6 cells onto VDP-coated glass 40 mm dishes and cultured for 2−4 days prior to staining and imaging.

***β*-Amyloid and Dextran Uptake Assay.** FAM-labeled β-amyloid peptide (Aβ-FAM 1−42; Anaspec) was reconstituted using a minimal volume of 1% NH_4OH and immediately diluted to a 1 mg/mL solution in PBS. Single-use aliquots were stored at −20 °C until use. For the uptake assay, astrocytes seeded in a 24 well plate were treated with 500−1000 nM Aβ-FAM, 50 μg/mL dextran-Alexa Fluor 647 (ThermoFisher), or both for 24 h. For flow cytometry, cells were washed with cold PBS and dissociated using trypsin (ThermoFisher) for 5 min at 37 °C to remove any surface-bound peptide. Samples were placed on ice and 5000−10000 live cells were analyzed on an Accuri C6 flow cytometer (BD Biosciences) to quantify median fluorescence intensity. For fluorescence microscopy, cells were imaged on a Nikon Ti2 Eclipse.

Cryopreservation of Differentiated Astrocytes. After a minimum of 45 days of differentiation, astrocytes that were 85% confluent were dissociated using Accutase and resuspended in cryopreservation medium. The cells were first gradually cooled to −80 °C in a Mr. Frosty freezing container (ThermoFisher) for 24 h, after which the vials were transferred to −150 °C for long-term storage. For the functional comparison experiments, astrocytes were thawed 7 days after freezing.

Statistical Analysis. Student's *t*-test and ANOVA were used to analyze the data, with a Bonferroni post hoc correction where

https://dx.doi.org/10.1021/acsbiomaterials.0c00067
ACS Biomater. Sci. Eng. 2020, 6, 3477−3490

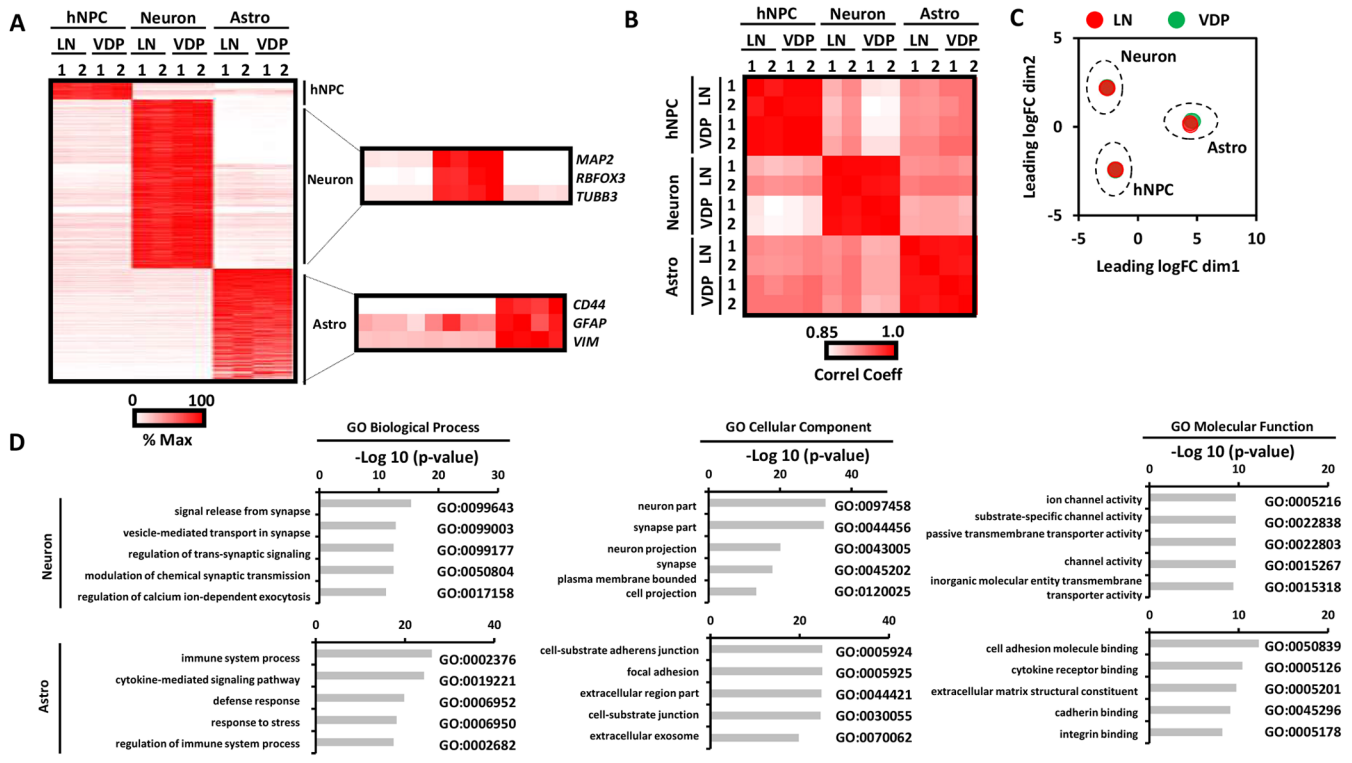

Figure 2. Transcriptional profiling of astrocytes generated on VDP and control LN surfaces. (A) Heat map for differentially expressed genes (FDR < 0.05; $|\log_2(\text{fold change})| > 1.5$) identified between NDC-1 derived hNPCs, astrocytes, and neurons cultured on VDP and LN surfaces. Genes related to postmitotic neurons and astrocytic phenotype are highlighted. The entire RNA-seq data set can be found in Supplementary Table 4 and the differentially expressed genes can be found in Supplementary Table 5. (B) Pearson's correlation between RNA-sequencing data of hNPCs, astrocytes, and neurons generated on VDP and LN substrates. (C) Multidimensional scaling (MDS) plot measuring differences in the transcriptional profiles of hNPCs, astrocytes, and neurons differentiated on VDP- and LN-coated surfaces. (D) Gene ontology (GO) analysis identified biological processes (left panels), cellular components (middle panels), and molecular function (right panels) that were upregulated in neuronal (top panels) and astrocyte (bottom panel) populations derived on both VDP- and LN-coated surfaces.

appropriate. Significance represents a p-value < 0.05. Additionally, all data are displayed as mean ± standard error of the mean (SEM) unless otherwise specified.

RESULTS

Highly Efficient Generation of Astrocytes from Multiple Independent hPSC Lines on a Defined Substrate. We previously described a protocol that employs a fully defined peptide-based substrate, referred to as vitronectin-derived peptide (VDP), that allows for the differentiation and long-term expansion of multipotent human neural progenitor cells (hNPCs).[35] To that end, we derived hNPCs from six independent hPSC lines (Supplementary Table 3), two lines from healthy nondemented control patients (herein referred to as NDC-1 and NDC-2), two lines from familial Alzheimer's disease patients (herein referred to as FAD-1 and FAD-2), and two lines from sporadic Alzheimer's disease patients (herein referred to as SAD-1 and SAD-2). Similar to our other established hNPC lines, all six hNPC lines expressed high levels of the canonical hNPC markers SOX1, SOX2, and NESTIN (Supplementary Figure 1). To determine if VDP could support the differentiation of hNPCs into functional astrocytes, hNPCs were seeded onto VDP or control animal-derived laminin (LN) (an extracellular matrix protein commonly used in astrocytic differentiation of hPSCs[17−20]) substrates, and the medium was changed from neural expansion medium (NEM) to astrocyte differentiation medium (ADM). HNPCs differentiated on both VDP and LN substrates rapidly acquired a flat, star-shaped astrocytic morphology (Figure 1A). By day 30, the majority of the cells (>90%) on both substrates acquired the astrocyte progenitor marker CD44[36] (Figure 1B). In addition, quantitative RT-PCR (qPCR) showed that expression of genes associated with an astrocytic phenotype such as *GFAP*[37] and *VIM*[38] was similar in astrocytes generated on VDP- and LN-coated surfaces (Figure 1C). Similarly, immunofluorescence (Figure 1D, Supplementary Figures 2−3) and flow cytometry (Figure 1E) demonstrated that a high percentage (>85%) of hNPCs cultured on VDP-coated surfaces expressed the astrocyte markers GFAP and S100β.[37] In sum, this data demonstrates that VDP can support the differentiation of hNPCs into astrocytes at an efficiency similar to that on conventional LN substrates.

Astrocytes Generated on LN and VDP Share a Similar Transcriptional Profile. To further characterize the extent to which astrocytes generated on VDP were similar to those differentiated on LN, we performed RNA-sequencing (RNA-seq) analysis on hNPCs, neurons, and astrocytes derived from NDC-1 hPSCs generated on VDP and LN substrates (Supplementary Table 4). Clustering (Figure 2A), correlation (Figure 2B), and multidimensional scaling (Figure 2C) analyses revealed that astrocytes generated on VDP and LN showed a high degree of similarity and grouped distinctly from the hNPC and neuronal cell populations. A closer examination of the genes statistically significantly upregulated ($\log_2$ FC > 1.5, FDR < 0.05; Supplementary Table 5) in the astrocytic

https://dx.doi.org/10.1021/acsbiomaterials.0c00067
ACS Biomater. Sci. Eng. 2020, 6, 3477−3490

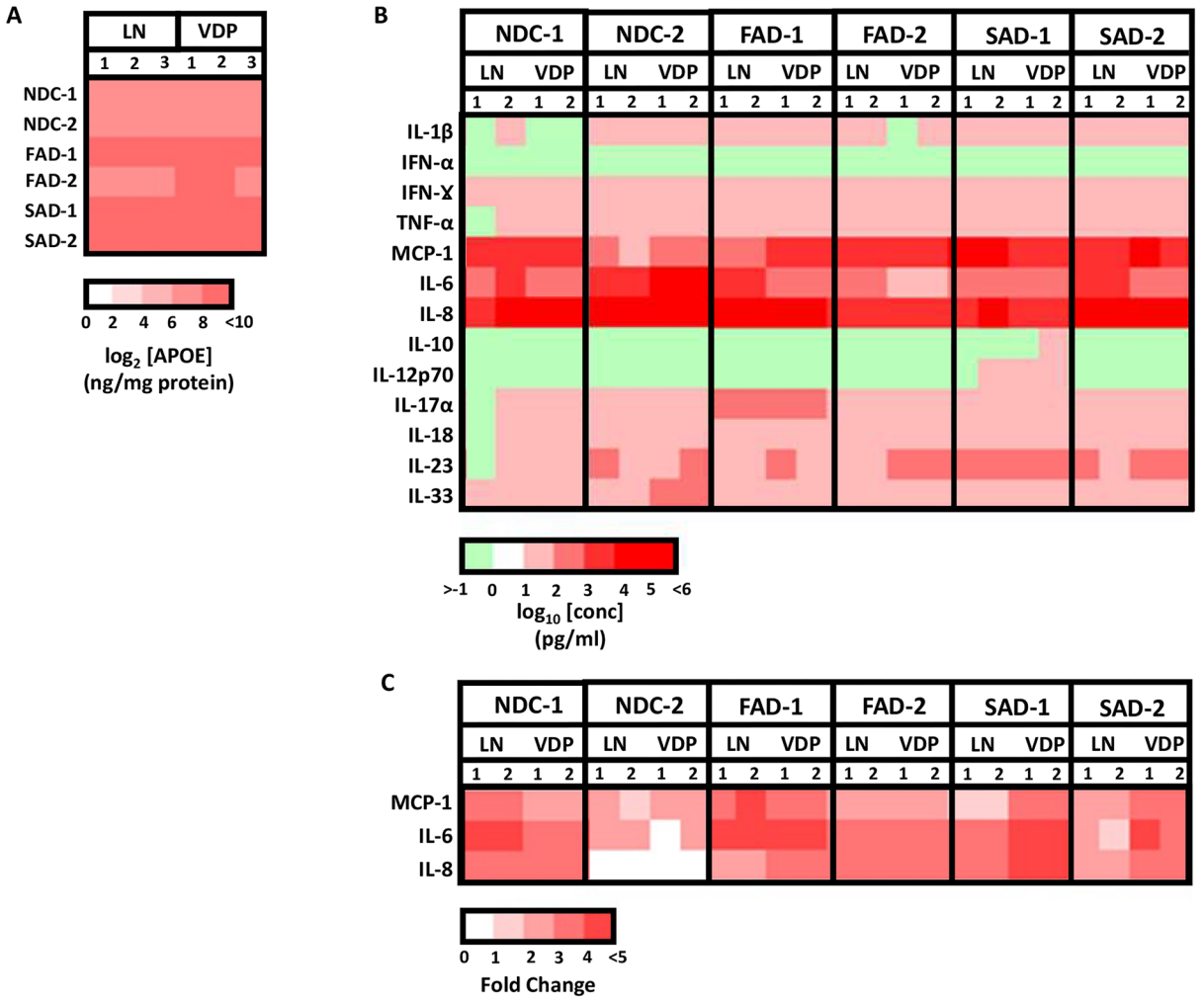

Figure 3. Secretory profiling of VDP- and LN-derived astrocytes. (A) ApoE secretion was measured in the conditioned medium of D50+ astrocytes. (B) Secretory profile of pro- and anti-inflammatory cytokines in D50+ astrocytes cultured under basal conditions. (C) D50+ astrocytes were treated with LPS for 24 h and the secretion of MCP-1, IL-6, and IL-8 was measured. Data is shown as fold-change increase in cytokine secretion when compared to untreated conditions.

populations revealed high levels of not only established astrocyte markers (e.g., *CD44*, *GFAP*, *NFIX*, *VIM*) but also processes associated with astrocytic function including growth factor production (e.g., *BDNF*, *CTGF*, *IGF2*, *TGFBI*), mediation of cell-adhesion (e.g., *ICAM1*, *ITGA1*, *ITGA5*, *ITGA6*, *ITGB1*, *ITGB3*, *ITGB5*), extracellular matrix secretion (e.g., *COLL11A1*, *FN1*, *LAMB2*, *TNC*), and inflammatory and immune response (e.g., *CCL2*, *IL1A*, *IL6*, *IL8*). In addition, astrocytes derived on both VDP and LN surfaces did not display significant levels of hNPC- (e.g., *SOX1*, *SOX2*) or neuronal-associated (e.g., *MAP2*, *RBFOX3*, *TUBB3*) markers. Gene ontology (GO) analysis further confirmed that genes upregulated in both VDP- and LN-derived astrocytes were related to typical astrocytic biological processes (e.g., immune system processes, cytokine-mediated signaling[39−42]), cellular components (e.g., cell substrate junction, focal adhesion[43−45]), and molecular functions (e.g., cadherin, cell adhesion molecule, and integrin binding[46,47]) (Figure 2D). On the other hand, GO analysis revealed that gene sets concomitantly downregulated in the astrocyte cell populations but upregulated in neuronal cells were typical of the biological processes, cellular components, and molecular functions of electrophysiologically active neurons. Overall, these results indicate that astrocytes generated on VDP substrates are not only transcriptionally indistinguishable from those derived on control LN substrates but have an expression profile that is characteristic of functional astrocytes.

VDP-Derived Astrocytes Secrete Robust Amounts of ApoE. Although the astrocytes generated on VDP expressed the genes and proteins typically associated with astrocytes, we next wanted to measure their functional characteristics. Apolipoprotein E (ApoE) is a lipoprotein transporter involved in cholesterol transport that is generated and secreted by functionally mature astrocytes.[48] In the brain, ApoE also plays important roles related to neuronal growth, synaptic plasticity, and membrane repair.[49,50] To determine whether astrocytes generated on VDP produced ApoE, we measured the amount of ApoE in the conditioned media by ELISA. Compared to hNPCs, which produced no detectable level of ApoE, astrocytes generated on both VDP and control LN substrates produced ApoE in the range of 50−150 ng/mg protein (Figure 3A), which is consistent with the levels of ApoE produced by hPSC-derived astrocytes in other studies.[28] In addition, there was no consistent difference between astrocytes generated on

https://dx.doi.org/10.1021/acsbiomaterials.0c00067
ACS Biomater. Sci. Eng. 2020, 6, 3477−3490

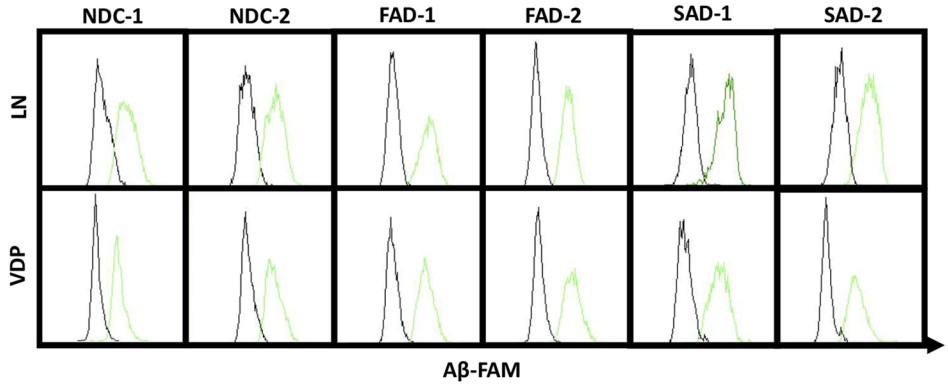

Figure 4. Analysis of β-amyloid (Aβ) uptake in astrocytes. Flow cytometry analysis of Aβ internalization in untreated (black traces) and Aβ-FITC-treated (green traces) astrocytes.

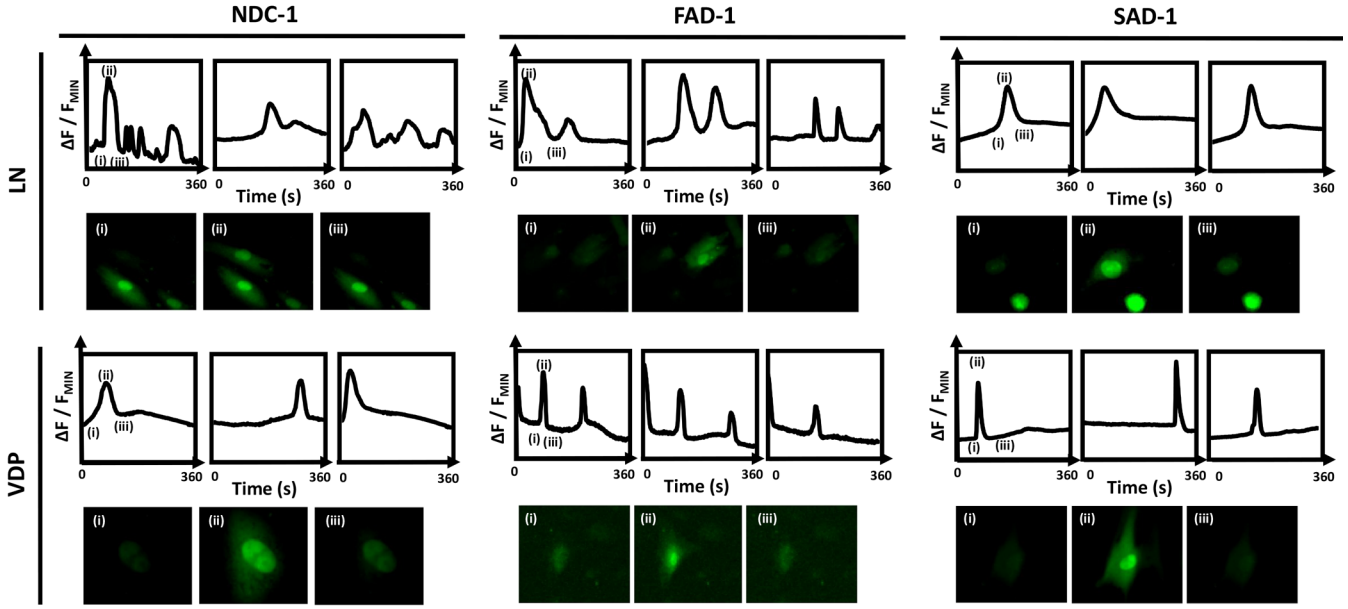

Figure 5. Measurement of spontaneous calcium activity in astrocytes differentiated on VDP- and LN-coated plates. Plots of changes ($\Delta F/F$) in fluorescence of calcium indicator (Fluo-4) in single astrocytic cells. Representative images of Fluo-4 stained astrocytes at the indicated time points.

VDP or LN surfaces in terms of levels of ApoE secretion. These results indicate that hPSC-derived astrocytes generated on VDP secrete robust and comparable amounts of ApoE to those astrocytes generated on LN control substrates.

Astrocytes Derived on VDP Are Responsive to Inflammatory Stimuli. Astrocytes play a chief role in the inflammatory response in the central nervous system through secretion of cytokines and growth factors that mediate tissue damage, repair, and survival.[41,51,52] Given the importance of astrocytes regulating the neuroinflammatory processes in the central nervous system in response to neurodegenerative disease, ischemia, or acute brain injury, we wanted to determine if astrocytes differentiated on VDP substrates were responsive to inflammatory stimuli. To that end, we utilized a cytokine bead array to measure the amount of inflammation-related cytokines in the conditioned media of astrocytes derived on VDP and control LN surfaces. In the absence of any stimulation, we found that astrocytes on VDP and LN secreted modest or undetectable levels of numerous pro-inflammatory (IFN-α, IL-1β, TNF-α, MCP-1, IL-6, IL-8, IL-10, IL-18, IL-23, IL-33) and anti-inflammatory cytokines (IFN-γ, IL-12, IL-17α) (Figure 3B), consistent with previous reports in primary and hPSC-derived astrocytes, which show low levels of such cytokines in unstimulated conditions.[34,42,53−57] In order to test if these astrocyte populations altered their cytokine secretion profile in response to inflammatory stimuli, we treated cell populations generated on both VDP and LN with lipopolysaccharide (LPS), a bacterial cell wall endotoxin widely used to study cellular responses to inflammation.[58−60] Across all astrocytic populations tested, we observed an increase of IL-6, IL-8, and MCP-1, which is consistent with previous studies in primary and hPSC-derived astrocytes showing that these cytokines are the prime mediators of the inflammatory response[34,53−55,61] (Figure 3C). Moreover, there was no obvious difference in the responses of VDP- or LN-derived astrocytes. Together, these findings indicate that astrocytes generated on VDP are capable of responding to inflammatory stimuli through modulation of their secreted cytokine profile.

VDP-Generated Astrocytes Have the Ability to Uptake Amyloid (Aβ). Amyloidogenic processing of the full-length transmembrane protein β-amyloid precursor protein (APP) is a multistage process that results in generation of Aβ

https://dx.doi.org/10.1021/acsbiomaterials.0c00067
ACS Biomater. Sci. Eng. 2020, 6, 3477−3490

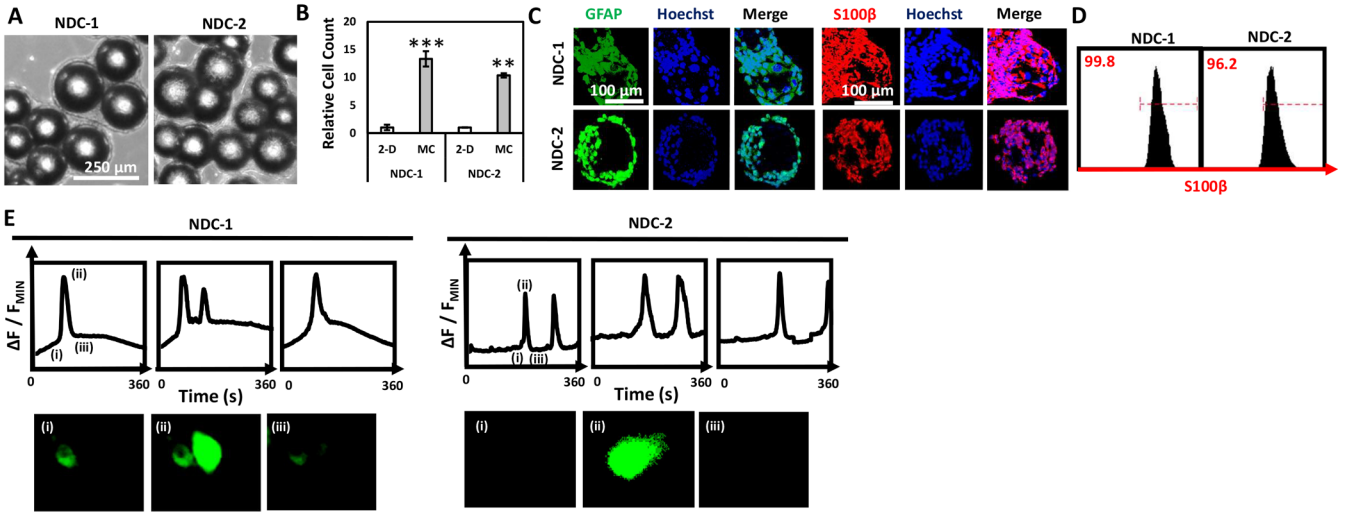

Figure 6. Scalable generation of hPSC-derived astrocytes on VDP-coated microcarriers (MCs). (A) Representative phase contrast images of astrocytes cultured on VDP-coated MCs (scale bar = 250 μm). (B) Cell counts of astrocytes generated on VDP-coated two-dimensional (2D) surfaces and MCs. Student's t test, $^{**}p < 0.01$, $^{***}p < 0.001$. (C) Representative fluorescent images of GFAP (left panels) and S100β (right panels) in astrocyte cultures derived on VDP-coated MCs (scale bar = 100 μm). (D) Representative flow cytometry plots of S100β expression of astrocytes derived on MCs. Gates were determined using isotype or secondary antibody only controls listed in Supplementary Table 1. (E) Plots of changes ($\Delta F/F$) in fluorescence of calcium indicator (Fluo-4) in single astrocytic cells grown on MCs. Inset images of Fluo-4 stained astrocytes are shown at the indicated time points.

peptides of various lengths, most commonly Aβ38, Aβ40, Aβ42.[62] Under healthy physiological conditions in the central nervous system, Aβ peptides play important roles related to synapse function and neuronal activity.[63,64] The levels of Aβ in the extracellular space are, in part, regulated by astrocytes which play a significant role in Aβ clearance.[65] To that end, to determine whether the astrocytes generated on VDP and LN surfaces were able to internalize Aβ, we treated astrocytes with FITC-conjugated Aβ(1−42) and measured uptake 24 h later with flow cytometry (Figure 4). In addition, fluorescent image analysis of astrocytes treated with FITC-Aβ and fluorescently labeled dextran confirms cell internalization of Aβ via the endosomal pathway (Supplementary Figure 4).

This analysis revealed that astrocytes generated on both substrates were capable of significant uptake of Aβ (Figure 4).

VDP-Generated Astrocytes Display Spontaneous Calcium Activity. A hallmark property of mature astrocytes is the ability to exhibit spontaneous calcium transients.[66−68] As such, we used Fluo-4AM to monitor calcium signaling in hPSC-derived astrocytes differentiated on VDP and control LN substrates in a subset of our lines, NDC-1, FAD-1, and SAD-1. We found that cells on both surfaces displayed spontaneous waves of calcium transients with characteristics similar to those in previous reports with primary or hPSC-derived astrocytes,[34,53,68] with no distinguishing features between those on VDP and those on LN (Figure 5). In addition, single cell quantification of the amplitudes of the calcium spikes revealed no obvious differences in the distribution of these responses among the cell populations on VDP and LN substrates (Supplementary Figure 5). Finally, astrocyte populations on both surfaces displayed continuous propagation of waves of calcium transients among neighboring cells suggesting networks of connected astrocytes (Supplementary Movies 1−6). Taken together, these results suggest that hPSC-derived astrocytes produced on VDP and LN substrates exhibit characteristic calcium responses typical of functionally mature cells.

Astrocytes Can Be Generated on VDP Using Scalable Culture Methods. Although we were able to employ VDP as a fully defined culture substrate for the generation of astrocytes, the inadequate surface area-to-volume ratio provided by such traditional two-dimensional (2D) methods is not sufficient to generate astrocytic cell populations in quantities sufficient for uses in disease modeling, drug discovery, and regenerative medicine. As an alternative, microcarrier (MC)-based technologies can facilitate the generation of large numbers of cells in reduced culture volumes.[69] More specifically, in microcarrier culture, cells are grown as monolayers on the surface of small polystyrene spheres of approximately 200 μm diameter while suspended in culture with mild stirring. Importantly, the flexibility of MCs allows them to be easily employed in a variety of bioreactor systems including stirred-tank, rotating wall vessel, and vertical wheel.[70,71] To that end, we developed a strategy to coat polystyrene MCs with VDP. As proof-of-principle, hNPCs derived from our two NDC hPSC lines were seeded onto the VDP-coated MCs in 6-well ultralow attachment plates. After seeding, the medium was changed to astrocyte differentiation medium. We optimized the initial seeding and MC density to allow for continuous attachment of cells and even distribution on the MCs through the differentiation period (Figure 6A). Differentiation on MCs allowed for a 10−15-fold increase in astrocyte cell number per culture volume when compared to conventional 2D culture methods (Figure 6B). In addition, immunofluorescent (Figure 6C) and flow cytometry (Figure 6D) analyses demonstrated that astrocytes generated on MCs expressed levels of the established astrocyte markers S100β and GFAP similar to those cells generated on typical 2D surfaces. Finally, calcium imaging was performed on astrocytes that were generated on VDP-coated MCs and then subsequently replated onto VDP-coated 2D surfaces. This analysis revealed

https://dx.doi.org/10.1021/acsbiomaterials.0c00067
ACS Biomater. Sci. Eng. 2020, 6, 3477−3490

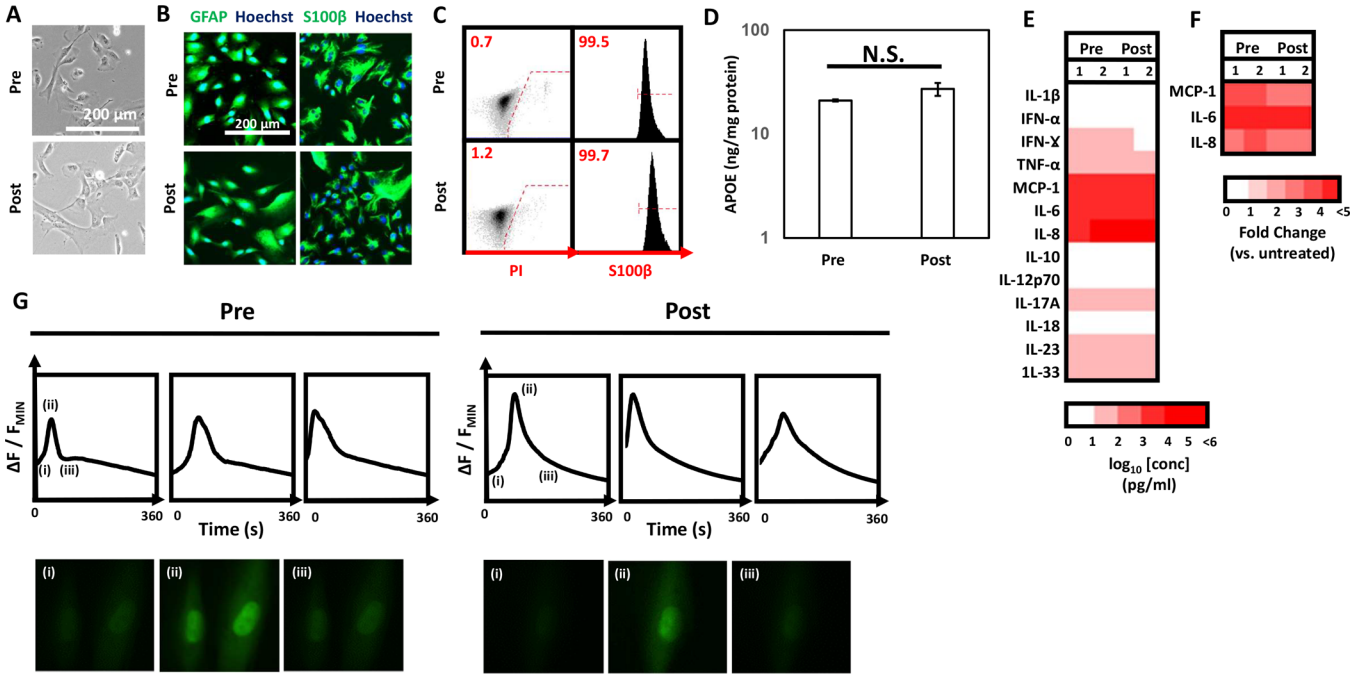

Figure 7. Characterization of cryopreserved astrocytes generated on VDP. (A) Representative phase contrast images of pre- and post-cryopreserved astrocytes generated on VDP-coated surfaces. (B) Representative immunofluorescent images of GFAP (left panels) and S100β (right panels) in pre- and post-cryopreserved astrocytes. (C) Representative flow cytometry plots of propidium iodide staining (left panel) and S100β expression (right panel) in pre- and postcryopreserved astrocytes. Gates were determined using isotype or secondary antibody only controls listed in Supplementary Table 1 as appropriate. (D) Measurement of secreted ApoE in pre- and post-cryopreserved astrocytes cultured on VDP surfaces. N.S. = not statistically significant, Student's t test. (E) Profile of pro- and anti-inflammatory cytokines in pre- and post-cryopreserved astrocytes cultured under basal conditions. (F) Measurement of upregulated cytokines in pre- and post-cryopreserved astrocytes after treatment with LPS. Data is shown as fold-change increase in cytokine release compared to untreated astrocytes. (G) Measurement of changes ($\Delta F/F$) in fluorescence of calcium indicator (Fluo-4) in single pre- and post-cryopreserved astrocytes. Inset images of Fluo-4 stained astrocytes are shown at the indicated time points.

that cells generated with the MC-based system displayed calcium transients with the same properties as those generated on 2D surfaces (Figure 6E; Supplementary Movies 7 and 8). Therefore, astrocytes generated with these scalable methods can be dissociated and replated onto VDP-coated 2D surfaces without loss of functionality. In sum, these experiments establish proof-of-principle that VDP is compatible with scalable culture methods to generate functionally mature astrocytes in quantities required for downstream applications.

Astrocytes Generated on VDP Can Be Cryopreserved without Loss of Functionality. Now that we established that VDP could be used to support the scalable generation of hPSC-derived astrocytes, we wanted to investigate if these cell populations could be cryopreserved while maintaining their functional phenotypes. As proof-of-principle, astrocytes were generated from NDC-1 hNPCs on VDP-coated surfaces, dissociated to single cell suspensions, and placed in a DMSO-based cryoprotectant. Cells were then cooled from room temperature at a rate of 1 °C/min to −80 °C and then placed in long-term storage at −150 °C. After a minimum of 7 days in storage, cells were thawed onto VDP-coated surfaces. Thawed astrocytes displayed a typical flat, star-shaped morphology that was similar to cells prior to cryopreservation (Figure 7A). In addition, cells that were cryopreserved continued to express high levels of the astrocytic markers S100β and GFAP as determined by immunofluorescence (Figure 7B, Supplementary Figure 6) and flow cytometry (Figure 7C). In addition, there was no significant difference in the levels of ApoE secreted between pre- and post-cryopreserved astrocytes (Figure 7D). Along similar lines, thawed astrocytes retained their characteristic secretory profile (Figure 7E) and retained the ability to respond to inflammatory stimuli such as LPS through upregulation of expression of cytokines IL-6, IL-8, and MCP-1 (Figure 7F). Finally, cryopreserved astrocytes continued to display spontaneous calcium transients with profiles similar to those of cells prior to cryopreservation (Figure 7G; Supplementary Movies 9 and 10). As a whole, these results demonstrate that not only can VDP provide for the scalable generation of hPSC-derived astrocytes but also that the resultant populations can be cryopreserved without any adverse effects on their functionality.

DISCUSSION

In the central nervous system (CNS), astrocytes play numerous roles to maintain the homeostasis of neural microenvironment such as regulating neurotransmitter levels in the interstitial tissue, supporting synaptic health and function, and modulating energy and lipid metabolism. More broadly, not only are astrocytes mediators of the systemic inflammatory and injury response in healthy tissue[4,5] but they also have been implicated as central players in numerous neurodegenerative diseases.[3] As such, hPSC-derived astrocytes provide a unique opportunity to generate accessible models to understand the molecular underpinnings of neurodegenerative disease as well as serve as the raw material to replace diseased or damaged tissue. In this vein, reproducible and defined methods for the generation of astrocytes from hPSCs will significantly advance their use in these various downstream

https://dx.doi.org/10.1021/acsbiomaterials.0c00067
ACS Biomater. Sci. Eng. 2020, 6, 3477−3490

applications.[6] To that end, in this study we employed a completely defined peptide-based substrate, vitronectin-derived peptide (VDP), for the efficient generation of astrocytes from hPSCs. Overall, the cells generated on these substrates not only expressed high levels of conventional astrocytic markers but also displayed transcriptional and functional characteristics consistent with hPSC-derived astrocytes generated by other groups on undefined xenogeneic substrates[28,34,53,54] (Supplementary Table 6) as well as fetal astrocytes and primary human astrocytes. Specifically, hPSC-derived astrocytes were generated from six independent hPSC lines and subject to a series of primary characterization assays that are broadly accepted in the field[34,53,54] as demonstration of bona fide astrocytes including morphological assessment, expression of high levels of astrocytic markers, ability to produce and secrete ApoE, and ability to take up soluble Aβ. In addition, we performed more in-depth characterization on a select number of lines of these hPSC-derived astrocytes using RNA-seq and calcium imaging. In the future, direct comparative investigations will be necessary to compare hPSC-derived astrocytes generated using the defined approaches described in this study with those isolated from fetal and primary sources. In addition, these astrocytes can also be evaluated in the context of other hiPSC-derived neural populations such as neurons[72] and microglia[73] to understand and model the complex interactions between these cell types. Furthermore, we demonstrated that VDP was compatible with microcarrier (MC)-based cell culture technologies to facilitate the large-scale generation of astrocytes from hPSCs. Finally, astrocytes generated on these defined substrates could be cryopreserved without adverse effects on functionality. Notably, VDP can be coated onto tissue-culture treated polystyrene plates or MCs and does not require complex chemical conjugation or fabrication that is typical of other peptide-based culture systems for growth or differentiation of hPSCs.[74,75] Because of this ease of use, we contend that VDP can be widely adopted by researchers as a defined substrate for the generation of hPSC-derived astrocytes for disease modeling and regenerative medicine applications.

Loss or dysfunction of astrocytes contributes to a wide variety of neurological disorders, including Huntington's disease, amyotrophic lateral sclerosis (ALS), epilepsy, and Alzheimer's disease (AD).[76,77] Recent preclinical studies have provided great enthusiasm for the potential of using hPSC-derived astrocytes in the treatment of numerous CNS diseases and disorders. For example, astrocytes generated from hPSCs have been shown to functionally replace astrocytes in adult mice.[78] More recently, intrathecal delivery of similar astrocyte populations into mouse models of ALS was able to mitigate disease onset and progression.[79] In this vein, the results presented here will enable the development of biomanufacturing processes with the following features that will be critical for the translation of hPSC-derived astrocytes from bench-to-bedside: (i) *Fully defined conditions.* Current astrocytic differentiation protocols exclusively employ substrates from xenogeneic origins,[16,18−20,78,80] which are subject to batch-to-batch variation and pose risk for transmission of adventitious agents in clinical situations.[21,22,81] As described in this study, the use of VDP provides a completely synthetic and off-the-shelf substrate to generate human induced pluripotent stem cell (hiPSC)-derived astrocytes in reproducible, animal-free conditions. In fact, we demonstrate that VDP allows for the generation of astrocytes that are transcriptionally and functionally indistinguishable from cells derived on conventional animal-derived substrates such as laminin (LN). (ii) *Robust.* It has been widely established that variability between individual hPSC lines can lead to directed differentiation protocols that work well in a subset of cell lines and, alternatively, lead to the generation of heterogeneous cell populations in other lines.[82,83] Here, we show that VDP provides for the highly efficient differentiation of six independent hiPSC lines into relatively pure, homogeneous astrocyte populations. In addition, we do not observe any significant differences in cell phenotype with independent VDP batches or independent differentiations. As such, we anticipate that VDP can serve as a universal substrate enabling the development of biomanufacturing processes and personalized therapies. (iii) *Scalable.* Current astrocyte differentiation strategies utilize planar culture surfaces that will not be able to facilitate the anticipated large-scale clinical demands of up to 10^9−10^{10} cells per dose. Alternatively, microcarrier (MC)-based systems have the ability to enhance production capacity, improve culture robustness, facilitate scale-up, and reduce costs associated with cell manufacturing.[69] Here, we use VDP in conjunction with a MC-based culture system to allow for the scalable generation of functionally mature hPSC-derived astrocytes. Although we only demonstrate the utility of this MC-based system in a subset of our hPSC lines, our proof-of-principle studies demonstrate the broad utility of VDP to be employed in such scalable formats with minimal optimization. In the future, we anticipate that such MC-based systems used in conjunction with established bioreactor systems[70,71] will allow for the production of astrocytes in quantities sufficient for cell-based therapy applications. More precisely, in the proof-of-principle experiments we performed, VDP-coated MCs were cultured in 6-well ultralow attachment plates placed on an orbital shaker in a tissue culture incubator. From this culture system, each well yielded on average 6×10^6 astrocytes compared to 0.5×10^6 astrocytes obtained from a single well when cultured using 2D. As such, we estimate that a single 500 mL vessel of a rotating wall vessel (RWV) bioreactor could be used to generate 10^9 astrocytes using VDP-coated MCs.[35] (iv) *Point-of-use.* Future clinical applications of astrocytes differentiated from hPSCs will require processes that are compatible with cryopreservation techniques that allow for the generation of master banks that can be deployed directly at the point-of-use.[21,22,81] Toward this goal, we provide proof-of-concept in a subset of our hPSC lines that the astrocyte populations generated on VDP can be dissociated into single cells and cryopreserved without any loss of phenotypical integrity and functionality for long-term study.

Recently, suspension or "organoid"-based methods have emerged as a strategy to generate neural cell populations, including astrocytes, in a format that might preclude an adhesive matrix.[29,84−88] It should be noted that while these organoid-based systems are impressive in their ability to recapitulate aspects of human neural development, in practical terms these protocols result in a heterogeneous mixture of neurons, astrocytes, and other neural progenitor cell types, which might limit downstream applications where pure cell populations are required. Specifically, organoid-based systems suffer from limitations such as batch-to-batch variability in size and cellular composition, as well as potential issues that arise from nectrotic cores that develop during prolonged culture. By comparison, the methods described in this study, which employ a fully defined substrate that is compatible with both

https://dx.doi.org/10.1021/acsbiomaterials.0c00067
ACS Biomater. Sci. Eng. 2020, 6, 3477−3490

conventional 2D and scalable MC-based culture systems, result in highly pure populations of astrocytes free from any contaminating (i.e., neuronal, progenitor) cell populations. In the future, such astrocytic populations could be combined at precise ratios with other hPSC-derived cell populations such as neurons[72] and microglia[73] to generate highly reproducible, complex culture systems. In addition, these organoid suspension culture systems rely on the aggregation of cells into large spheroids which might result in cell necrosis in the center of the organoid due to limitations in oxygen diffusion and nutrient mass transfer.[89] In this study, the MC-based cultures form small aggregates with a noncellular MC core that does not exhibit necrosis. In fact, analysis of astrocytes generated on MCs revealed no observable necrosis as measured by propidium iodide staining.[90] As such, the MC-based methods described in this study offer the scalability advantages afforded by suspension-based systems without these aforementioned caveats.

The work that we performed in this study also has important practical implications for the use of hPSC-derived astrocytes in disease modeling and drug screening applications. In particular, cellular models for phenotypic drug screens need to be reproducible and homogeneous.[54,91] In addition, such cell types will need to be generated at large scale given the estimates that it would take approximately 10^{10} cells to screen a 1 million compound library. The use of VDP as a fully defined synthetic substrate to generate relatively pure and homogeneous astrocytes from hPSCs will eliminate the batch-to-batch variability that could arise from the use of animal-derived substrates. Moreover, VDP does not pose the same potential complications as undefined matrices such as Matrigel, which might contain biologically active components that could potentially interfere with the interpretation of phenotypic results.[92,93] In addition, we demonstrate that the use of scalable MC-based technologies and conventional cryopreservation techniques will enable the generation of large stocks of consistent cellular identity. In turn, we show that cryopreserved cells can be thawed directly onto VDP-coated 2D surfaces, which will enable future downstream high-throughput phenotypic drug screening assays.

Classically, the roles of astrocytes in CNS function and neurodegenerative disease have been studied in a variety of animal models. While these model systems have provided many insights, the complexity of *in vivo* experiments make it difficult to eliminate confounding variables and directly investigate the specific role of astrocytes in neural tissue health, damage, and disease. In addition, given the differences between human and rodent astrocytes including their morphology, transcriptional profiles, and functionality,[94−96] there is significant concern that these models do not fully recapitulate human disease. As such, considerable effort has been devoted to developing representative human *in vitro* astrocytic models including those from immortalized[97,98] and primary sources.[96,99] However, immortalized cell lines can be aneuploid with unknown dosage of key disease relevant genes, while primary cell systems are difficult to isolate and rapidly lose phenotypes during prolonged *in vitro* culture. In this vein, the hPSC-astrocytes generated in this study have many functional features that would make them attractive for AD-related disease modeling and drug screening. In the classic form of the amyloid cascade hypothesis of AD, generation and subsequent accumulation of Aβ peptides is the key step that leads to neuronal loss and subsequent cognitive decline associated with AD.[62,100,101] Related to this process, astrocytes have been shown to play an important role in Aβ clearance.[65] In this study, we demonstrated that astrocytes generated on VDP had the ability to take up Aβ from the surrounding media. Moving forward, the cells generated as part of this study will provide for the investigation into the mechanistic connections between astrocytic amyloid processing and AD-related phenotypes. Another characteristic of the astrocytes generated as part of this study that makes them attractive drug screening models is their ability to secrete ApoE. Given the broad functions of ApoE in maintaining health in the CNS,[102] augmenting the functions of ApoE has been explored as a potential therapeutic strategy in treating AD.[97,98] As such, several screens utilizing immortalized and primary cell sources have identified small molecule enhancers of ApoE production.[97,98] Moving forward, the astrocytes generated in this work could serve as a more robust human cellular model for such high-throughput screens. Finally, although the work presented in this manuscript only focused on the generation of astrocytes from nondemented control (NDC) or AD hiPSCs, we envision that the robustness of the VDP-based culture methods will allow for the generation of astrocytes from other hiPSC lines derived from patients of other diseases in which astrocytic dysfunction has been implicated.[76,77]

CONCLUSION

In summary, we developed a completely defined peptide-based substrate that allows for the generation of highly pure populations of astrocytes from several independent hPSC lines. Moreover, this peptide is compatible with conventional planar culture formats as well as scalable MC-based technologies. Importantly, astrocytes generated on these peptide-based surfaces not only displayed typical astrocytic morphology and high expression of canonical astrocyte markers but also demonstrated properties characteristic of functionally mature cells including secretion of ApoE, responsiveness to inflammatory stimuli, and presentation of spontaneous calcium transients. In the future, the use of this peptide-based system as a scalable and defined culture system will enable the application of hPSC-derived astrocytes in a variety of downstream applications in drug screening, disease modeling, and regenerative medicine.

ASSOCIATED CONTENT

Supporting Information

The Supporting Information is available free of charge at https://pubs.acs.org/doi/10.1021/acsbiomaterials.0c00067.

Complete RNA-seq data set for hNPCs, neurons, and astrocytes generated on VDP- and LN-coated surfaces (XLSX)

List of genes that are expressed at statistically (FDR < 0.05, fold change > 1.5) different levels in RNA-seq data set (XLSX)

Supplementary Movie 1, representative recording of fluorescent calcium transients in NDC-1 astrocytes derived on VDP-coated substrates (MP4)

Supplementary Movie 2, representative recording of fluorescent calcium transients in NDC-1 astrocytes derived on LN-coated substrates (MP4)

Supplementary Movie 3, representative recording of fluorescent calcium transients in FAD-1 astrocytes derived on VDP-coated substrates (MP4)

https://dx.doi.org/10.1021/acsbiomaterials.0c00067
ACS Biomater. Sci. Eng. 2020, 6, 3477−3490

Supplementary Movie 4, representative recording of fluorescent calcium transients in FAD-1 astrocytes derived on LN-coated substrates (MP4)
Supplementary Movie 5, representative recording of fluorescent calcium transients in SAD-1 astrocytes derived on VDP-coated substrates (MP4)
Supplementary Movie 6, representative recording of fluorescent calcium transients in SAD-1 astrocytes derived on LN-coated substrates (MP4)
Supplementary Movie 7, representative recording of fluorescent calcium transients in NDC-1 astrocytes derived on VDP-coated MCs (MP4)
Supplementary Movie 8, representative recording of fluorescent calcium transients in NDC-2 astrocytes derived on VDP-coated MCs (MP4)
Supplementary Movie 9, representative recording of fluorescent calcium transients in NDC-1 astrocytes pre-cryopreservation (MP4)
Supplementary Movie 10, representative recording of fluorescent calcium transients in NDC-1 astrocytes post-cryopreservation (MP4)
Characterization of hNPCs used in this study by immunofluorescence of hNPC markers SOX1, SOX2, and NESTIN, immunofluorescence analysis for expression of GFAP in D50+ cultures, immunofluorescence analysis for expression of S100β in D50+ cultures, fluorescence imaging analysis of β-amyloid (Aβ) uptake in astrocytes, analysis of calcium transients in single astrocytic cells derived on VDP- and LN-coated substrates, immunofluorescent images of GFAP and S100β in pre- and postcryopreserved astrocytes, list of antibodies used in this study, list of qPCR primers used in this study, description of hPSC lines used in this study, and comparison of phenotypic characterization of astrocytes in this study with astrocytes generated in previous studies using undefined xenogeneic substrates (PDF)

AUTHOR INFORMATION

Corresponding Author

David A. Brafman − *School of Biological and Health Systems Engineering, Arizona State University, Tempe, Arizona 85287, United States;* orcid.org/0000-0001-6131-2532; Phone: (480) 727-2859; Email: David.Brafman@asu.edu

Authors

Sreedevi Raman − *School of Biological and Health Systems Engineering, Arizona State University, Tempe, Arizona 85287, United States*

Gayathri Srinivasan − *School of Biological and Health Systems Engineering, Arizona State University, Tempe, Arizona 85287, United States*

Nicholas Brookhouser − *School of Biological and Health Systems Engineering, Arizona State University, Tempe, Arizona 85287, United States; Graduate Program in Clinical Translational Sciences, University of Arizona College of Medicine-Phoenix, Phoenix, Arizona 85004, United States*

Toan Nguyen − *School of Biological and Health Systems Engineering, Arizona State University, Tempe, Arizona 85287, United States*

Tanner Henson − *School of Biological and Health Systems Engineering, Arizona State University, Tempe, Arizona 85287, United States*

Daylin Morgan − *School of Biological and Health Systems Engineering, Arizona State University, Tempe, Arizona 85287, United States*

Joshua Cutts − *School of Biological and Health Systems Engineering, Arizona State University, Tempe, Arizona 85287, United States*

Complete contact information is available at: https://pubs.acs.org/10.1021/acsbiomaterials.0c00067

Author Contributions

[§]S.R., G.S., and N.B. contributed equally to this work.

Notes

The authors declare no competing financial interest.

ACKNOWLEDGMENTS

Funding for this work was provided by the NIH-NIBIB (5R21EB020767) and NIH-NIA (5R21AG056706). N.B. was supported by a fellowship from the International Foundation for Ethical Research. Imaging was performed at the Regenerative Medicine and Bioimaging Facility at Arizona State University using instrumentation acquired by the NIH SIG award 1 S10 RR027154-01A1. Research was sponsored by the Office of the Secretary of Defense and was accomplished under Agreement Number W911NF-17-3-001. The views and conclusions contained in this document are those of the authors and should not be interpreted as representing the official policies, either expressed or implied, of the Office of the Secretary of Defense or the U.S. Government. The U.S. Government is authorized to reproduce and distribute reprints for Government purposes notwithstanding any copyright notation herein.

REFERENCES

(1) Oberheim, N. A.; Wang, X.; Goldman, S.; Nedergaard, M. Astrocytic Complexity Distinguishes the Human Brain. *Trends Neurosci.* **2006**, *29* (10), 547−553.
(2) De Pittà, M.; Brunel, N.; Volterra, A. Astrocytes: Orchestrating Synaptic Plasticity? *Neuroscience* **2016**, *323*, 43−61.
(3) Sofroniew, M. V.; Vinters, H. V. Astrocytes: Biology and Pathology. *Acta Neuropathol.* **2010**, *119*, 7−35.
(4) Khakh, B. S.; Sofroniew, M. V. Diversity of Astrocyte Functions and Phenotypes in Neural Circuits. *Nat. Neurosci.* **2015**, *18* (7), 942−952.
(5) Zhang, Y.; Barres, B. A. Astrocyte Heterogeneity: An Underappreciated Topic in Neurobiology. *Curr. Opin. Neurobiol.* **2010**, *20* (5), 588−594.
(6) Gonzalez, D. M.; Gregory, J.; Brennand, K. J. The Importance of Non-Neuronal Cell Types in HiPSC-Based Disease Modeling and Drug Screening. *Front. Cell Dev. Biol.* **2017**, *5*, 117.
(7) Pei, Y.; Peng, J.; Behl, M.; Sipes, N. S.; Shockley, K. R.; Rao, M. S.; Tice, R. R.; Zeng, X. Comparative Neurotoxicity Screening in Human IPSC-Derived Neural Stem Cells, Neurons and Astrocytes. *Brain Res.* **2016**, *1638*, 57−73.
(8) Oksanen, M.; Lehtonen, S.; Jaronen, M.; Goldsteins, G.; Hämäläinen, R. H.; Koistinaho, J. Astrocyte Alterations in Neurodegenerative Pathologies and Their Modeling in Human Induced Pluripotent Stem Cell Platforms. *Cell. Mol. Life Sci.* **2019**, *76* (14), 2739−2760.
(9) Izrael, M.; Slutsky, S. G.; Admoni, T.; Cohen, L.; Granit, A.; Hasson, A.; Itskovitz-Eldor, J.; Krush Paker, L.; Kuperstein, G.; Revel, M.; et al. Safety and Efficacy of Human Embryonic Stem Cell-Derived Astrocytes Following Intrathecal Transplantation in SOD1G93A and NSG Animal Models. *Stem Cell Res. Ther.* **2018**, *9* (1), 152.

(10) Kokaia, Z.; Llorente, I. L.; Carmichael, S. T. Customized Brain Cells for Stroke Patients Using Pluripotent Stem Cells. *Stroke* **2018**, *49* (5), 1091−1098.
(11) Wang, S.-M.; Lee, C.-U.; Lim, H. K. Stem Cell Therapies for Alzheimer's Disease: Is It Time? *Curr. Opin. Psychiatry* **2019**, *32* (2), 105−116.
(12) Hunsberger, J.; Lundberg, M. S.; Allickson, J.; Simon, C. G.; Zylberberg, C.; Beachy, S. H. Examining Resources, Initiatives, and Regulatory Pathways to Advance Regenerative Medicine Manufacturing. *Curr. Stem Cell Reports* **2019**, *5* (4), 162−172.
(13) Aijaz, A.; Li, M.; Smith, D.; Khong, D.; LeBlon, C.; Fenton, O. S.; Olabisi, R. M.; Libutti, S.; Tischfield, J.; Parekkadan, B.; et al. Biomanufacturing for Clinically Advanced Cell Therapies. *Nat. Biomed. Eng.* **2018**, *2* (6), 362−376.
(14) Shariatzadeh, M.; Chandra, A.; Wilson, S. L.; McCall, M. J.; Morizur, L.; Lesueur, L.; Chose, O.; Gepp, M. M.; Schulz, A.; Williams, D. J.; et al. Distributed Automated Manufacturing of Pluripotent Stem Cell Products. *Int. journal, Adv. Manuf. Technol.* **2020**, *106* (3), 1085−1103.
(15) Hunsberger, J. G.; Shupe, T.; Atala, A. An Industry-Driven Roadmap for Manufacturing in Regenerative Medicine. *Stem Cells Transl. Med.* **2018**, *7* (8), 564−568.
(16) Serio, A.; Bilican, B.; Barmada, S. J.; Ando, D. M.; Zhao, C.; Siller, R.; Burr, K.; Haghi, G.; Story, D.; Chandran, S.; et al. Astrocyte Pathology and the Absence of Non-Cell Autonomy in an Induced Pluripotent Stem Cell Model of TDP-43 Proteinopathy. *Proc. Natl. Acad. Sci. U. S. A.* **2013**, *110* (12), 4697−4702.
(17) Haidet-Phillips, A. M.; Roybon, L.; Gross, S. K.; Tuteja, A.; Donnelly, C. J.; Richard, J.-P.; Ko, M.; Sherman, A.; Eggan, K.; Henderson, C. E.; Maragakis, N. J.; et al. Gene Profiling of Human Induced Pluripotent Stem Cell-Derived Astrocyte Progenitors Following Spinal Cord Engraftment. *Stem Cells Transl. Med.* **2014**, *3* (5), 575−585.
(18) Roybon, L.; Lamas, N. J.; Garcia-Diaz, A.; Yang, E. J.; Sattler, R.; Jackson-Lewis, V.; Kim, Y. A.; Kachel, C. A.; Rothstein, J. D.; Henderson, C. E.; et al. Human Stem Cell-Derived Spinal Cord Astrocytes with Defined Mature or Reactive Phenotypes. *Cell Rep.* **2013**, *4* (5), 1035−1048.
(19) Krencik, R.; Weick, J. P.; Liu, Y.; Zhang, Z.-J.; Zhang, S.-C. Specification of Transplantable Astroglial Subtypes from Human Pluripotent Stem Cells. *Nat. Biotechnol.* **2011**, *29* (6), 528−534.
(20) Shaltouki, A.; Peng, J.; Liu, Q.; Rao, M. S.; Zeng, X. Efficient Generation of Astrocytes from Human Pluripotent Stem Cells in Defined Conditions. *Stem Cells* **2013**, *31* (5), 941−952.
(21) De Sousa, P. A.; Downie, J. M.; Tye, B. J.; Bruce, K.; Dand, P.; Dhanjal, S.; Serhal, P.; Harper, J.; Turner, M.; Bateman, M. Development and Production of Good Manufacturing Practice Grade Human Embryonic Stem Cell Lines as Source Material for Clinical Application. *Stem Cell Res.* **2016**, *17* (2), 379−390.
(22) Stacey, G. N.; Andrews, P. W.; Barbaric, I.; Boiers, C.; Chandra, A.; Cossu, G.; Csontos, L.; Frith, T. J.; Halliwell, J. A.; Wagey, R.; et al. Stem Cell Culture Conditions and Stability: A Joint Workshop of the PluriMes Consortium and Pluripotent Stem Cell Platform. *Regener. Med.* **2019**, *14* (3), 243−255.
(23) Simaria, A. S.; Hassan, S.; Varadaraju, H.; Rowley, J.; Warren, K.; Vanek, P.; Farid, S. S. Allogeneic Cell Therapy Bioprocess Economics and Optimization: Single-Use Cell Expansion Technologies. *Biotechnol. Bioeng.* **2014**, *111* (1), 69−83.
(24) Silva, M. M.; Rodrigues, A. F.; Correia, C.; Sousa, M. F. Q.; Brito, C.; Coroadinha, A. S.; Serra, M.; Alves, P. M. Robust Expansion of Human Pluripotent Stem Cells: Integration of Bioprocess Design With Transcriptomic and Metabolomic Characterization. *Stem Cells Transl. Med.* **2015**, *4* (7), 731−742.
(25) Silva, M.; Daheron, L.; Hurley, H.; Bure, K.; Barker, R.; Carr, A. J.; Williams, D.; Kim, H.-W.; French, A.; Wall, I.; et al. Generating IPSCs: Translating Cell Reprogramming Science into Scalable and Robust Biomanufacturing Strategies. *Cell Stem Cell* **2015**, *16* (1), 13−17.
(26) Lin, H.; Li, Q.; Lei, Y. An Integrated Miniature Bioprocessing for Personalized Human Induced Pluripotent Stem Cell Expansion and Differentiation into Neural Stem Cells. *Sci. Rep.* **2017**, *7* (1), 40191.
(27) Varun, D.; Srinivasan, G. R.; Tsai, Y.-H.; Kim, H.-J.; Cutts, J.; Petty, F.; Merkley, R.; Stephanopoulos, N.; Dolezalova, D.; Marsala, M.; Brafman, D. A. A Robust Vitronectin-Derived Peptide for the Scalable Long-Term Expansion and Neuronal Differentiation of Human Pluripotent Stem Cell (HPSC)-Derived Neural Progenitor Cells (HNPCs). *Acta Biomater.* **2017**, *48*, 120−130.
(28) Zhao, J.; Davis, M. D.; Martens, Y. A.; Shinohara, M.; Graff-Radford, N. R.; Younkin, S. G.; Wszolek, Z. K.; Kanekiyo, T.; Bu, G. APOE E4/E4 Diminishes Neurotrophic Function of Human IPSC-Derived Astrocytes. *Hum. Mol. Genet.* **2017**, *26* (14), 2690−2700.
(29) Paşca, A. M.; Sloan, S. A.; Clarke, L. E.; Tian, Y.; Makinson, C. D.; Huber, N.; Kim, C. H.; Park, J.-Y.; O'Rourke, N. A.; Paşca, S. P.; et al. Functional Cortical Neurons and Astrocytes from Human Pluripotent Stem Cells in 3D Culture. *Nat. Methods* **2015**, *12* (7), 671−678.
(30) Dobin, A.; Davis, C. A.; Schlesinger, F.; Drenkow, J.; Zaleski, C.; Jha, S.; Batut, P.; Chaisson, M.; Gingeras, T. R. STAR: Ultrafast Universal RNA-Seq Aligner. *Bioinformatics* **2013**, *29* (1), 15−21.
(31) Liao, Y.; Smyth, G. K.; Shi, W. FeatureCounts: An Efficient General Purpose Program for Assigning Sequence Reads to Genomic Features. *Bioinformatics* **2014**, *30* (7), 923−930.
(32) Robinson, M. D.; McCarthy, D. J.; Smyth, G. K. EdgeR: A Bioconductor Package for Differential Expression Analysis of Digital Gene Expression Data. *Bioinformatics* **2010**, *26* (1), 139−140.
(33) Huang, D. W.; Sherman, B. T.; Lempicki, R. A. Systematic and Integrative Analysis of Large Gene Lists Using DAVID Bioinformatics Resources. *Nat. Protoc.* **2009**, *4* (1), 44−57.
(34) TCW, J.; Wang, M.; Pimenova, A. A.; Bowles, K. R.; Hartley, B. J.; Lacin, E.; Machlovi, S. I.; Abdelaal, R.; Karch, C. M.; Brennand, K. J.; et al. An Efficient Platform for Astrocyte Differentiation from Human Induced Pluripotent Stem Cells. *Stem Cell Rep.* **2017**, *9* (2), 600−614.
(35) Srinivasan, G.; Morgan, D.; Varun, D.; Brookhouser, N.; Brafman, D. A. An Integrated Biomanufacturing Platform for the Large-Scale Expansion and Neuronal Differentiation of Human Pluripotent Stem Cell-Derived Neural Progenitor Cells. *Acta Biomater.* **2018**, *74*, 168−179.
(36) Liu, Y.; Han, S. S. W.; Wu, Y.; Tuohy, T. M. F.; Xue, H.; Cai, J.; Back, S. A.; Sherman, L. S.; Fischer, I.; Rao, M. S. CD44 Expression Identifies Astrocyte-Restricted Precursor Cells. *Dev. Biol.* **2004**, *276* (1), 31−46.
(37) Ludwin, S. K.; Kosek, J. C.; Eng, L. F. The Topographical Distribution of S-100 and GFA Proteins in the Adult Rat Brain: An Immunohistochemical Study Using Horseradish Peroxidase-Labelled Antibodies. *J. Comp. Neurol.* **1976**, *165* (2), 197−207.
(38) Schnitzer, J.; Franke, W. W.; Schachner, M. Immunocytochemical Demonstration of Vimentin in Astrocytes and Ependymal Cells of Developing and Adult Mouse Nervous System. *J. Cell Biol.* **1981**, *90* (2), 435−447.
(39) Dong, Y.; Benveniste, E. N. Immune Function of Astrocytes. *Glia* **2001**, *36* (2), 180−190.
(40) Guerriero, F.; Sgarlata, C.; Francis, M.; Maurizi, N.; Faragli, A.; Perna, S.; Rondanelli, M.; Rollone, M.; Ricevuti, G. Neuro-inflammation, Immune System and Alzheimer Disease: Searching for the Missing Link. *Aging Clin. Exp. Res.* **2017**, *29* (5), 821−831.
(41) Colombo, E.; Farina, C. Astrocytes: Key Regulators of Neuroinflammation. *Trends Immunol.* **2016**, *37* (9), 608−620.
(42) Sofroniew, M. V. Multiple Roles for Astrocytes as Effectors of Cytokines and Inflammatory Mediators. *Neuroscientist* **2014**, *20* (2), 160−172.
(43) Wiese, S.; Karus, M.; Faissner, A. Astrocytes as a Source for Extracellular Matrix Molecules and Cytokines. *Front. Pharmacol.* **2012**, *3*, 120.
(44) Cho, S.; Muthukumar, A. K.; Stork, T.; Coutinho-Budd, J. C.; Freeman, M. R. Focal Adhesion Molecules Regulate Astrocyte

Morphology and Glutamate Transporters to Suppress Seizure-like Behavior. *Proc. Natl. Acad. Sci. U. S. A.* **2018**, *115* (44), 11316−11321.
(45) Moeton, M.; Stassen, O. M. J. A.; Sluijs, J. A.; van der Meer, V. W. N.; Kluivers, L. J.; van Hoorn, H.; Schmidt, T.; Reits, E. A. J.; van Strien, M. E.; Hol, E. M. GFAP Isoforms Control Intermediate Filament Network Dynamics, Cell Morphology, and Focal Adhesions. *Cell. Mol. Life Sci.* **2016**, *73* (21), 4101−4120.
(46) Liddelow, S.; Hoyer, D. Astrocytes: Adhesion Molecules and Immunomodulation. *Curr. Drug Targets* **2016**, *17* (16), 1871−1881.
(47) Hillen, A. E. J.; Burbach, J. P. H.; Hol, E. M. Cell Adhesion and Matricellular Support by Astrocytes of the Tripartite Synapse. *Prog. Neurobiol.* **2018**, *165*−*167*, 66−86.
(48) Hauser, P. S.; Ryan, R. O. Impact of Apolipoprotein E on Alzheimer's Disease. *Curr. Alzheimer Res.* **2013**, *10* (8), 809−817.
(49) Suri, S.; Heise, V.; Trachtenberg, A. J.; Mackay, C. E. The Forgotten APOE Allele: A Review of the Evidence and Suggested Mechanisms for the Protective Effect of APOE ε2. *Neurosci. Biobehav. Rev.* **2013**, *37* (10), 2878−2886.
(50) Lane-Donovan, C.; Herz, J. ApoE, ApoE Receptors, and the Synapse in Alzheimer's Disease. *Trends Endocrinol. Metab.* **2017**, *28* (4), 273−284.
(51) Sofroniew, M. V. Astrocyte Barriers to Neurotoxic Inflammation. *Nat. Rev. Neurosci.* **2015**, *16* (5), 249−263.
(52) Liddelow, S. A.; Barres, B. A. Reactive Astrocytes: Production, Function, and Therapeutic Potential. *Immunity* **2017**, *46* (6), 957−967.
(53) Santos, R.; Vadodaria, K. C.; Jaeger, B. N.; Mei, A.; Lefcochilos-Fogelquist, S.; Mendes, A. P. D. D.; Erikson, G.; Shokhirev, M.; Randolph-Moore, L.; Gage, F. H.; et al. Differentiation of Inflammation-Responsive Astrocytes from Glial Progenitors Generated from Human Induced Pluripotent Stem Cells. *Stem Cell Rep.* **2017**, *8* (6), 1757−1769.
(54) Lundin, A.; Delsing, L.; Clausen, M.; Ricchiuto, P.; Sanchez, J.; Sabirsh, A.; Ding, M.; Synnergren, J.; Zetterberg, H.; Falk, A.; et al. Human IPS-Derived Astroglia from a Stable Neural Precursor State Show Improved Functionality Compared with Conventional Astrocytic Models. *Stem Cell Rep.* **2018**, *10* (3), 1030−1045.
(55) Perriot, S.; Mathias, A.; Perriard, G.; Canales, M.; Jonkmans, N.; Merienne, N.; Meunier, C.; El Kassar, L.; Perrier, A. L.; Du Pasquier, R.; et al. Human Induced Pluripotent Stem Cell-Derived Astrocytes Are Differentially Activated by Multiple Sclerosis-Associated Cytokines. *Stem Cell Rep.* **2018**, *11* (5), 1199−1210.
(56) van Neerven, S.; Regen, T.; Wolf, D.; Nemes, A.; Johann, S.; Beyer, C.; Hanisch, U.-K.; Mey, J. Inflammatory Chemokine Release of Astrocytes in Vitro Is Reduced by All-Trans Retinoic Acid. *J. Neurochem.* **2010**, *114* (5), 1511−1526.
(57) Choi, S. S.; Lee, H. J.; Lim, I.; Satoh, J.; Kim, S. U. Human Astrocytes: Secretome Profiles of Cytokines and Chemokines. *PLoS One* **2014**, *9* (4), No. e92325.
(58) Strokin, M.; Sergeeva, M.; Reiser, G. Proinflammatory Treatment of Astrocytes with Lipopolysaccharide Results in Augmented Ca2+ Signaling through Increased Expression of via Phospholipase A2 (IPLA2). *Am. J. Physiol. Cell Physiol.* **2011**, *300* (3), C542−9.
(59) Zamanian, J. L.; Xu, L.; Foo, L. C.; Nouri, N.; Zhou, L.; Giffard, R. G.; Barres, B. A. Genomic Analysis of Reactive Astrogliosis. *J. Neurosci.* **2012**, *32* (18), 6391−6410.
(60) Hamby, M. E.; Coppola, G.; Ao, Y.; Geschwind, D. H.; Khakh, B. S.; Sofroniew, M. V. Inflammatory Mediators Alter the Astrocyte Transcriptome and Calcium Signaling Elicited by Multiple G-Protein-Coupled Receptors. *J. Neurosci.* **2012**, *32* (42), 14489−14510.
(61) Martinez, M.; Modric, S. Patient Variation in Veterinary Medicine: Part I. Influence of Altered Physiological States. *J. Vet. Pharmacol. Ther.* **2010**, *33* (3), 213−226.
(62) Oksanen, M.; Petersen, A. J.; Naumenko, N.; Puttonen, K.; Lehtonen, Š.; Gubert Olivé, M.; Shakirzyanova, A.; Leskelä, S.; Sarajärvi, T.; Koistinaho, J.; et al. PSEN1Mutant IPSC-Derived Model Reveals Severe Astrocyte Pathology in Alzheimer's Disease. *Stem Cell Rep.* **2017**, *9* (6), 1885−1897.
(63) Vallée, A.; Lecarpentier, Y. Alzheimer Disease: Crosstalk between the Canonical Wnt/Beta-Catenin Pathway and PPARs Alpha and Gamma. *Front. Neurosci.* **2016**, *10*, 459.
(64) Palop, J. J.; Mucke, L. Amyloid-Beta-Induced Neuronal Dysfunction in Alzheimer's Disease: From Synapses toward Neural Networks. *Nat. Neurosci.* **2010**, *13* (7), 812−818.
(65) Ries, M.; Sastre, M. Mechanisms of Aβ Clearance and Degradation by Glial Cells. *Front. Aging Neurosci.* **2016**, *8*, 160.
(66) Levin, E. D.; McGurk, S. R.; Rose, J. E.; Butcher, L. L. Reversal of a Mecamylamine-Induced Cognitive Deficit with the D2 Agonist, LY 171555. *Pharmacol., Biochem. Behav.* **1989**, *33* (4), 919−922.
(67) Shigetomi, E.; Patel, S.; Khakh, B. S. Probing the Complexities of Astrocyte Calcium Signaling. *Trends Cell Biol.* **2016**, *26* (4), 300−312.
(68) Volterra, A.; Liaudet, N.; Savtchouk, I. Astrocyte Ca^{2+} Signalling: An Unexpected Complexity. *Nat. Rev. Neurosci.* **2014**, *15* (5), 327−335.
(69) Badenes, S. M.; Fernandes-Platzgummer, A.; Rodrigues, C. A. V.; Diogo, M. M.; da Silva, C. L.; Cabral, J. M. S. Microcarrier Culture Systems for Stem Cell Manufacturing. *Stem Cell Manuf.* **2016**, 77−104.
(70) Abraham, E.; Ahmadian, B. B.; Holderness, K.; Levinson, Y.; McAfee, E. Platforms for Manufacturing Allogeneic, Autologous and IPSC Cell Therapy Products: An Industry Perspective. *Adv. Biochem. Eng./Biotechnol.* **2017**, *165*, 323−350.
(71) Maartens, J. H.; De-Juan-Pardo, E.; Wunner, F. M.; Simula, A.; Voelcker, N. H.; Barry, S. C.; Hutmacher, D. W. Challenges and Opportunities in the Manufacture and Expansion of Cells for Therapy. *Expert Opin. Biol. Ther.* **2017**, *17* (10), 1221−1233.
(72) D'Souza, G. X.; Rose, S. E.; Knupp, A.; Nicholson, D. A.; Keene, C. D.; Young, J. E. The Application of in Vitro-Derived Human Neurons in Neurodegenerative Disease Modeling. *J. Neurosci. Res.* **2020**, DOI: 10.1002/jnr.24615.
(73) Hirbec, H.; Déglon, N.; Foo, L. C.; Goshen, I.; Grutzendler, J.; Hangen, E.; Kreisel, T.; Linck, N.; Muffat, J.; Escartin, C.; et al. Emerging Technologies to Study Glial Cells. *GLIA* **2020**, DOI: 10.1002/glia.23780.
(74) Melkoumian, Z.; Weber, J. L.; Weber, D. M.; Fadeev, A. G.; Zhou, Y.; Dolley-Sonneville, P.; Yang, J.; Qiu, L.; Priest, C. A.; Brandenberger, R.; et al. Synthetic Peptide-Acrylate Surfaces for Long-Term Self-Renewal and Cardiomyocyte Differentiation of Human Embryonic Stem Cells. *Nat. Biotechnol.* **2010**, *28* (6), 606−610.
(75) Deng, Y.; Zhang, X.; Zhao, Y.; Liang, S.; Xu, A.; Gao, X.; Deng, F.; Fang, J.; Wei, S. Peptide-Decorated Polyvinyl Alcohol/Hyaluronan Nanofibers for Human Induced Pluripotent Stem Cell Culture. *Carbohydr. Polym.* **2014**, *101*, 36−39.
(76) Molofsky, A. V.; Krenick, R.; Ullian, E.; Tsai, H.; Deneen, B.; Richardson, W. D.; Barres, B. A.; Rowitch, D. H. Astrocytes and Disease: A Neurodevelopmental Perspective. *Genes Dev.* **2012**, *26* (9), 891−907.
(77) Scuderi, C.; Stecca, C.; Iacomino, A.; Steardo, L. Role of Astrocytes in Major Neurological Disorders: The Evidence and Implications. *IUBMB Life* **2013**, *65* (12), 957−961.
(78) Chen, H.; Qian, K.; Chen, W.; Hu, B.; Blackbourn, L. W.; Du, Z.; Ma, L.; Liu, H.; Knobel, K. M.; Ayala, M.; Zhang, S.-C. Human-Derived Neural Progenitors Functionally Replace Astrocytes in Adult Mice. *J. Clin. Invest.* **2015**, *125* (3), 1033−1042.
(79) Wang, Y.; Cheng, J.; Xie, D.; Ding, X.; Hou, H.; Chen, X.; Er, P.; Zhang, F.; Zhao, L.; Qian, D.; et al. NS1-Binding Protein Radiosensitizes Esophageal Squamous Cell Carcinoma by Transcriptionally Suppressing c-Myc. *Cancer Commun. (London, England)* **2018**, *38* (1), 33.
(80) Haidet-Phillips, A. M.; Roybon, L.; Gross, S. K.; Tuteja, A.; Donnelly, C. J.; Richard, J.-P.; Ko, M.; Sherman, A.; Eggan, K.; Henderson, C. E.; Maragakis, N. J. Gene Profiling of Human Induced Pluripotent Stem Cell-Derived Astrocyte Progenitors Following Spinal Cord Engraftment. *Stem Cells Transl. Med.* **2014**, *3* (5), 575−585.

(81) Stacey, G.; Andrews, P.; Asante, C.; Barbaric, I.; Barry, J.; Bisset, L.; Braybrook, J.; Buckle, R.; Chandra, A.; Williams, D.; et al. Science-Based Assessment of Source Materials for Cell-Based Medicines: Report of a Stakeholders Workshop. *Regener. Med.* **2018**, *13* (8), 935−944.
(82) Ortmann, D.; Vallier, L. Variability of Human Pluripotent Stem Cell Lines. *Curr. Opin. Genet. Dev.* **2017**, *46*, 179−185.
(83) Nishizawa, M.; Chonabayashi, K.; Nomura, M.; Tanaka, A.; Nakamura, M.; Inagaki, A.; Nishikawa, M.; Takei, I.; Oishi, A.; Yoshida, Y.; et al. Epigenetic Variation between Human Induced Pluripotent Stem Cell Lines Is an Indicator of Differentiation Capacity. *Cell Stem Cell* **2016**, *19* (3), 341−354.
(84) Lancaster, M. A.; Renner, M.; Martin, C.-A.; Wenzel, D.; Bicknell, L. S.; Hurles, M. E.; Homfray, T.; Penninger, J. M.; Jackson, A. P.; Knoblich, J. A. Cerebral Organoids Model Human Brain Development and Microcephaly. *Nature* **2013**, *501* (7467), 373−379.
(85) Huch, M.; Koo, B.-K. Modeling Mouse and Human Development Using Organoid Cultures. *Development* **2015**, *142* (18), 3113−3125.
(86) Di Lullo, E.; Kriegstein, A. R. The Use of Brain Organoids to Investigate Neural Development and Disease. *Nat. Rev. Neurosci.* **2017**, *18* (10), 573−584.
(87) Kelava, I.; Lancaster, M. A. Dishing out Mini-Brains: Current Progress and Future Prospects in Brain Organoid Research. *Dev. Biol.* **2016**, *420* (2), 199−209.
(88) Krencik, R.; Zhang, S.-C. Directed Differentiation of Functional Astroglial Subtypes from Human Pluripotent Stem Cells. *Nat. Protoc.* **2011**, *6* (11), 1710−1717.
(89) Kinney, M. A.; Sargent, C. Y.; McDevitt, T. C. The Multiparametric Effects of Hydrodynamic Environments on Stem Cell Culture. *Tissue Eng., Part B* **2011**, *17* (4), 249−262.
(90) Crowley, L. C.; Marfell, B. J.; Scott, A. P.; Waterhouse, N. J. Quantitation of Apoptosis and Necrosis by Annexin V Binding, Propidium Iodide Uptake, and Flow Cytometry. *Cold Spring Harb. Protoc.* **2016**, *2016* (11), pdb.prot087288.
(91) Thorne, N.; Malik, N.; Shah, S.; Zhao, J.; Class, B.; Aguisanda, F.; Southall, N.; Xia, M.; McKew, J. C.; Rao, M.; Zheng, W. High-Throughput Phenotypic Screening of Human Astrocytes to Identify Compounds That Protect Against Oxidative Stress. *Stem Cells Transl. Med.* **2016**, *5* (5), 613−627.
(92) Astashkina, A.; Mann, B.; Grainger, D. W. A Critical Evaluation of in Vitro Cell Culture Models for High-Throughput Drug Screening and Toxicity. *Pharmacol. Ther.* **2012**, *134* (1), 82−106.
(93) Hughes, C. S.; Postovit, L. M.; Lajoie, G. A. Matrigel: A Complex Protein Mixture Required for Optimal Growth of Cell Culture. *Proteomics* **2010**, *10* (9), 1886−1890.
(94) Oberheim, N. A.; Takano, T.; Han, X.; He, W.; Lin, J. H. C.; Wang, F.; Xu, Q.; Wyatt, J. D.; Pilcher, W.; Nedergaard, M.; et al. Uniquely Hominid Features of Adult Human Astrocytes. *J. Neurosci.* **2009**, *29* (10), 3276−3287.
(95) Tarassishin, L.; Suh, H.-S.; Lee, S. C. LPS and IL-1 Differentially Activate Mouse and Human Astrocytes: Role of CD14. *Glia* **2014**, *62* (6), 999−1013.
(96) Zhang, Y.; Sloan, S. A.; Clarke, L. E.; Caneda, C.; Plaza, C. A.; Blumenthal, P. D.; Vogel, H.; Steinberg, G. K.; Edwards, M. S. B.; Barres, B. A.; et al. Purification and Characterization of Progenitor and Mature Human Astrocytes Reveals Transcriptional and Functional Differences with Mouse. *Neuron* **2016**, *89* (1), 37−53.
(97) Fan, J.; Zareyan, S.; Zhao, W.; Shimizu, Y.; Pfeifer, T. A.; Tak, J.-H.; Isman, M. B.; Van den Hoven, B.; Duggan, M. E.; Kulic, I.; et al. Identification of a Chrysanthemic Ester as an Apolipoprotein E Inducer in Astrocytes. *PLoS One* **2016**, *11* (9), No. e0162384.
(98) Finan, G. M.; Realubit, R.; Chung, S.; Lütjohann, D.; Wang, N.; Cirrito, J. R.; Karan, C.; Kim, T.-W. Bioactive Compound Screen for Pharmacological Enhancers of Apolipoprotein E in Primary Human Astrocytes. *Cell Chem. Biol.* **2016**, *23* (12), 1526−1538.
(99) Malik, N.; Wang, X.; Shah, S.; Efthymiou, A. G.; Yan, B.; Heman-Ackah, S.; Zhan, M.; Rao, M. Comparison of the Gene Expression Profiles of Human Fetal Cortical Astrocytes with Pluripotent Stem Cell Derived Neural Stem Cells Identifies Human Astrocyte Markers and Signaling Pathways and Transcription Factors Active in Human Astrocytes. *PLoS One* **2014**, *9* (5), No. e96139.
(100) Chow, V. W.; Mattson, M. P.; Wong, P. C.; Gleichmann, M. An Overview of APP Processing Enzymes and Products. *NeuroMol. Med.* **2010**, *12* (1), 1−12.
(101) Zhang, Y.; Thompson, R.; Zhang, H.; Xu, H. APP Processing in Alzheimer's Disease. *Mol. Brain* **2011**, *4* (1), 3.
(102) Liu, C.-C.; Kanekiyo, T.; Xu, H.; Bu, G. Apolipoprotein E and Alzheimer Disease: Risk, Mechanisms and Therapy. *Nat. Rev. Neurol.* **2013**, *9* (2), 106−118.

https://dx.doi.org/10.1021/acsbiomaterials.0c00067
ACS Biomater. Sci. Eng. 2020, 6, 3477−3490